International Journal of Mass Spectrometry 281 (2009) 1–7

Contents lists available at ScienceDirect

International Journal of Mass Spectrometry

journal homepage: www.elsevier.com/locate/ijms

Electroless plating of silver nanoparticles on porous silicon for laser desorption/ionization mass spectrometry

Hong Yan [a], Ning Xu [a], Wen-Yi Huang [a], Huan-Mei Han [a], Shou-Jun Xiao [a,b,*]

[a] State Key Laboratory of Coordination Chemistry, School of Chemistry and Chemical Engineering, Nanjing National Laboratory of Microstructures, Nanjing University, Nanjing 210093, PR China
[b] State Key Laboratory of Bioelectronics, Southeast University, Nanjing 210096, PR China

ARTICLE INFO

Article history:
Received 4 August 2008
Received in revised form 30 October 2008
Accepted 31 October 2008
Available online 12 November 2008

Keywords:
Silver nanoparticles
4-Aminothiophenol
Self-assembled monolayer
Laser desorption/ionization mass spectrometry

ABSTRACT

An improved DIOS (desorption ionization on porous silicon) method for laser desorption/ionization mass spectrometry (LDI MS) by electroless plating of silver nanoparticles (AgNPs) on porous silicon (PSi) was developed. By addition of 4-aminothiophenol (4-ATP) into the $AgNO_3$ plating solution, the plating speed can be slowed down and simultaneously 4-ATP self-assembled monolayers (SAMs) on AgNPs (4-ATP/AgNPs) were formed. Both AgNPs and 4-ATP/AgNPs coated PSi substrates present much higher stability, sensitivity and reproducibility for LDI MS than the un-treated porous silicon ones. Their shelf life in air was tested for several weeks to a month and their mass spectra still displayed the same high quality and sensitivity as the freshly prepared ones. And more 4-ATP SAMs partly play a role of matrix to increase the ionization efficiency. A small organic molecule of tetrapyridinporphyrin (TPyP), oligomers of polyethylene glycol (PEG 400 and 2300), and a peptide of oxytocin were used as examples to demonstrate the feasibility of the silver-plated PSi as a matrix-free-like method for LDI MS. This approach can obtain limits of detection to femtomoles for TPyP, subpicomoles for oxytocin, and picomoles for PEG 400 and 2300, comparable to the traditional matrix method and much better than the DIOS method. It simplifies the sample preparation as a matrix-free-like method without addition of matrix molecules and homogenizes the sample spread over the spot for better and more even mass signals.

1. Introduction

Matrix-assisted laser desorption/ionization time-of-flight mass spectrometry (MALDI TOF MS), one of the most important soft ionization mass spectrometries, has become a powerful tool in mass analysis of proteins, DNAs, polymers, and small chemical compounds. In MALDI, a major function of the matrix is to absorb energy from the laser to fuel a dynamic process that brings sample molecules into the gas phase [1]. However, the use of a matrix introduces a number of problems into the analytical method. First, the analyte must be miscible with the matrix and they must form a homogeneous co-crystallized film. This requirement has made MALDI somewhat difficult to implement because the selection of the proper matrix is often a matter of trial and error. Furthermore, the co-crystallization process can be probably disrupted by some contaminants such as salts or surfactants and thus produce an uneven distribution of analytes in co-crystals, which causes so called 'sweet spot' (good mass signals of the analyte) and 'dead spot' (weak or no mass signals of the analyte) to occur. In addition, MALDI is rarely used for analysis of analytes with low molecular weight (<1000 m/z) because the matrix and matrix clusters typically have low molecular weight and interfere with the analysis of small analytes [2].

Because of the above limitations, a significant amount of work has been paid to develop new laser desorption ionization (LDI) techniques. Among them, the surface-assisted laser desorption/ionization mass spectrometry (SALDI MS) attracts much attention. The SALDI technique utilizes substrates, which generally do not significantly desorb with analytes together, to bring analytes to be desorbed and ionized. Many effective SALDI-assisted materials have also been discovered [3–38], such as pencil lead [3], carbon nanotubes [4–9], porous silicon [10–13], metal and metal oxide powders [14–28]. One of the most widely used SALDI substrates is porous silicon. DIOS has been applied to analysis of analytes ranging in molecular weight size from 150 to 12,000 Da as a matrix-free method over years [10]. In this technique, porous silicon traps analytes in the pores and on the surface, and also

* Corresponding author at: State Key Laboratory of Coordination Chemistry, School of Chemistry and Chemical Engineering, Nanjing National Laboratory of Microstructures, Nanjing University, Nanjing 210093, PR China.
Tel.: +86 25 83621001; fax: +86 25 83314502.
E-mail address: sjxiao@nju.edu.cn (S.-J. Xiao).

1387-3806/$ – see front matter © 2008 Elsevier B.V. All rights reserved.
doi:10.1016/j.ijms.2008.10.026

partly absorbs the laser energy and transfers it to the sample compounds to vaporize and ionize them. However, the chemical instability of porous silicon degrades the properties of the substrate and therefore additional handling procedures are required, although some of these issues have been overcome through surface modifications [12].

Nanoparticles, such as cobalt, gold and silver nanoparticles [14,15,20–28], have been demonstrated to be effective SALDI assisted materials for the analysis of small organic molecules. For example, metal nanoparticles were suspended in some vacuum-stable liquid as a matrix for LDI to enhance the ion yield of non-volatile analytes, SAMs modified noble metal nanoparticles were used as affinity-capture functionalities for enrichment and detection [24–26] and as matrix monolayers to aid the laser desorption/ionization of target molecules [27,28].

From the above review, we consider that metal-deposited PSi should be a good candidate substrate for LDI. Actually, the deposition of metals, such as Ag, Au, Pd, Cu, Pt and Ni on PSi has been investigated in the past few years for applications on microelectronics and on surface-enhanced Raman scattering (SERS) [39]. Besides physical deposition techniques, in which mainly the surface of PSi is metallized by sputtering and vacuum evaporation, several chemical methods have been developed in order to create metal micro- and nano-crystallites in the pores and on the top surface of PSi as well. The electroless plating procedure is simple: the PSi chip is submerged in solutions of metal salts, and the metal ions are reduced by hydrosilicon species into neutral metal particles within the PSi template, where PSi acts both as a reducing agent and as a template substrate for particle deposition [40]. SERS on silver-plated PSi has been applied to identify chemicals and biomolecules very efficiently for chemical and bio-sensing. Not only does the freshly silver-deposited PSi can efficiently enhance signals of Raman scattering, but also is it a substrate that can be stored for 10 days in air still displaying high sensitivity [41]. In our work, we employed both AgNPs and 4-ATP/AgNPs coated PSi surfaces as substrates for LDI. The morphology of deposited silver particles was characterized by scanning electron microscopy (SEM) to be at the range of 20–50 nm. The 4-ATP SAMs adsorbed on silver was evidenced by transmission infrared Fourier-transform (FTIR) spectra. Four samples, PEG oligomers with two different molecular weights (PEG 400 and PEG 2300), a small organic molecule of TPyP (m/z 618), and a small peptide of oxytocin (m/z 1007), were used as model compounds to demonstrate the feasibility of this technique. This approach can obtain limits of detection to femtomoles for TPyP, subpicomoles for oxytocin, and picomoles for PEG 400 and 2300, comparable to the traditional matrix method and much better than the DIOS method. And it simplifies the sample preparation as a matrix-free-like method without addition of matrix molecules and homogenizes the sample spread over the spot for better and more even mass signals. The shelf life of 4-ATP/AgNPs coated PSi in air was tested for up to a month and their mass spectra still displayed the same high quality and sensitivity as the freshly prepared ones.

2. Experimental

2.1. Instrumentation

A scanning electron microscope (S-4800, Hitachi, Japan) was used to observe surface topographical structures at an accelerating voltage of 15.0 kV. Stamps were not sputtered with gold prior to imaging. The images were obtained by a magnification of 100,000.

Transmission Fourier-transform infrared spectra were obtained with a Bruker IFS66/S spectrometer at 4 cm^{-1} resolution. The samples were mounted in a dry-air purged chamber. Background spectra were recorded by the use of a flat untreated and cleaned Si ⟨1 0 0⟩ wafer. The absorbance mode was used for recording IR spectra. Typically 32 scans were acquired per spectrum.

The laser desorption/ionization measurements were performed in a Bruker Reflex II MALDI-TOF mass spectrometer. This instrument is equipped with a delayed ion extraction device with 100 ns delay time and a pulsed nitrogen laser operated at 337 nm. The analyte ions were accelerated at 20 kV. All spectra were recorded in reflectron and positive ion mode. All spectra were averaged over 50 discrete laser shots except for PEG 2300 over 100 shots. The laser power was adjusted slightly above the threshold for the desorption/ionization process. All data were processed using Bruker Daltonics FlexAnalysis 2.4.

2.2. Chemicals and reagents

Silicon wafers (⟨1 0 0⟩, 3", p-type, boron-doped, 5.0–8.0 Ω cm, 500 μm thick) were purchased from Guangwei Electronic Material Co., Ltd (Shanghai, China). PEG 400 and α-cyano-4-hydroxycinnamic acid (CHCA) were obtained from Aldrich (America) and PEG 2300 from JenKem Technology Co., Ltd., (Beijing, China). Oxytocin was kindly provided by Prof. Tang of the Institute of Molecular Medicine at Nanjing Univ. and TPyP by Prof. Shen in the State Key Laboratory of Coordination Chemistry at Nanjing Univ. Silver nitrate (AR) was purchased from Boshen Chemical Co., Ltd. (Shanghai, China) and 4-ATP from Zhejiang Shou & Fu Chemical Co., Ltd. (China). Other reagents were reagent grade or higher and used as received unless otherwise specified and MILLI Q water (>18 MΩ) was used for all experiments.

2.3. Sample preparation

The Si wafers were cut into 1.5 cm × 1.5 cm squares, cleaned with 3:1 (v/v) H_2SO_4–H_2O_2 for 30 min (Notice: piranha solution reacts violently with organic materials and should be handled with extreme care), rinsed with copious amounts of water and absolute ethanol, and then immersed in water prior to the etching procedure. The square wafers were placed in a Teflon etching cell using a piece of aluminum foil as a back contact and a small O-ring to seal the wafer to the cell. The cell was filled with a 3:1 (v/v) mixture of 40% aqueous HF and absolute ethanol and a platinum mesh was immersed in the solution as the counter electrode. The etching process was lasted for 10 min in the dark with a constant anodic current of 60 mA/cm^2. After etching, the wafer was removed from the cell, washed with absolute ethanol and dried under a stream of nitrogen. While pipetting the sample solution of PEG 400 and PEG 2300 onto our freshly prepared PSi substrate directly, we did not detect any analyte ions and PEG-related ions. It indicates that the DIOS method needs careful screening of the silicon wafer resources and the etching parameters for some specific molecules. However the silver-plated PSi surface presents much higher tolerance for many kinds of molecules.

Three different substrate preparation methods were used, and they will be referred to as methods A, B, and C. In method A, the freshly etched PSi was immersed in an aqueous solution of 5 mmol/L silver nitrate for 20 s. The sample was then removed from the solution, washed with copious amounts of water and dried under a stream of nitrogen. The original dark-red colored PSi surface was coated with a bright silver film. In methods B and C, 4-ATP was added in the solution, in order to retard the reduction rate and also to be chemisorbed on AgNPs partly as a matrix for LDI. A mixture of 5 mmol/L silver nitrate in water ($AgNO_3/H_2O$), 10 mmol/L 4-ATP in ethanol (4-ATP/EtOH), and 1% trifluoroacetic acid (TFA) with volume ratio 10:5:4 (pH 1–2) was prepared and used for meth-

ods B and C. The freshly etched PSi was incubated in the mixture for 100 min and therefore the prepared substrate was referred to method B. During the plating process, large amounts of gas bubbles were observed. The solution turned into dark-brown. The sample was then removed and rinsed with water and dried under nitrogen. To speed up the plating process, sonication was operated at the beginning of incubation and plating was ended in 10 min, which was referred to method C. If required, the prepared substrates were further stored in a 1% TFA solution containing 10 mM 4-ATP in order to keep a well-organized 4-ATP SAMs. For substrates prepared by either method B or C, the bright silver film can stay in air for a long time up to a month or even longer with no influence on the mass signals of sample molecules.

The PSi substrates prepared by methods A, B, and C were mounted onto a specifically fabricated MALDI sample holder using double-side conductive adhesive tape. The analyte PEG was dissolved in acetonitrile (3 mmol/L), TPyP in dichloromethane (1 mmol/L) and oxytocin in MILLI Q water (1 mmol/L). And they were diluted to what required for determining the detection limits. A 1 μL solution was dropped onto the silver film of the substrate, air-dried, and the chip was introduced immediately into the mass spectrometer for measurements.

3. Results and discussion

The AgNPs were deposited in the pores and on the surface of PSi via reduction of Ag^+ by metastable hydrosilicon species [40]. The SEM images of AgNPs produced with methods A, B, and C were illustrated in Fig. 1(a)–(c), respectively. Method A produced discrete and submonolayered AgNPs in Fig. 1(a), with a typical size distribution between 30 and 60 nm (a few smaller and larger particles were also observed). Method B generated much smaller and relatively homogenous nanoparticles in Fig. 1(b) with diameters of 20–30 nm. These nanoparticles were densely packed and stacked to three dimensions. Considering the much longer plating process of 100 min, we believe that 4-ATP retards the particle growth, in accordance with a report which used the 4-ATP solution to prepare AgNPs [42]. On the other hand, it is known that thiol groups from 4-ATP and silver ions produce Ag–S-complexes at low pH values. This complexation effect decreases the oxidation potential between Ag and Ag^+ and induces a slow and well-proportional deposition. In method C, sonication accelerates the reaction and deposition rate and shortens the preparation time. A silver layer with nanoparticle size and surface coverage between methods A and B was generated.

The thiol compound like 4-ATP will cover the AgNPs to form a strong Ag–S-bonded monolayer during incubation. The monolayer was confirmed with a transmission FTIR. Fig. 2 shows the spectra of adsorbed 4-ATP monolayer. Three prominent absorption bands were observed at 1488, 1591, and 1623 cm^{-1}, which are assigned to the benzene ring vibration bands (1488: CC stretching + CH bending; 1591: CC stretching) and the NH bending band (1623 cm^{-1}), respectively. It also can be seen that the signal of 4-ATP from method B is stronger than from method C, which indicates larger amounts of AgNPs on the substrate fabricated by method B than by method C.

Four typical compounds, PEG 400, PEG 2300, TPyP, and oxytocin, were tested on all silver-deposited PSi layers for LDI MS analyses. The sample was spotted and spread homogeneously on the surface, and no solid crystals were observed under the microscope, which indicated formation of a homogeneous analyte overlayer. The chemical background mostly comes up in the low mass range less than m/z 400. The ions produced by silver correspond to silver clusters of Ag^+ (m/z 107), Ag_2^+ (m/z 215), and Ag_3^+ (m/z 322) in the spectra of PEG 400 in Fig. 3. They all are located in the low-mass region, and for the normal measurement concentrations (i.e., with nanomole samples) no clusters in the high mass region (>m/z 400) were observed. Sodium and potassium ions and others which cannot be exactly assigned also contribute to the chemical background in the range m/z 0–200. Although the intensity of the background ions increases strongly as the laser power increases, these ions are constant and reproducible. Therefore, the substrate-related background in the low-mass region can be easily distinguished from the analyte ions in the mass spectrum.

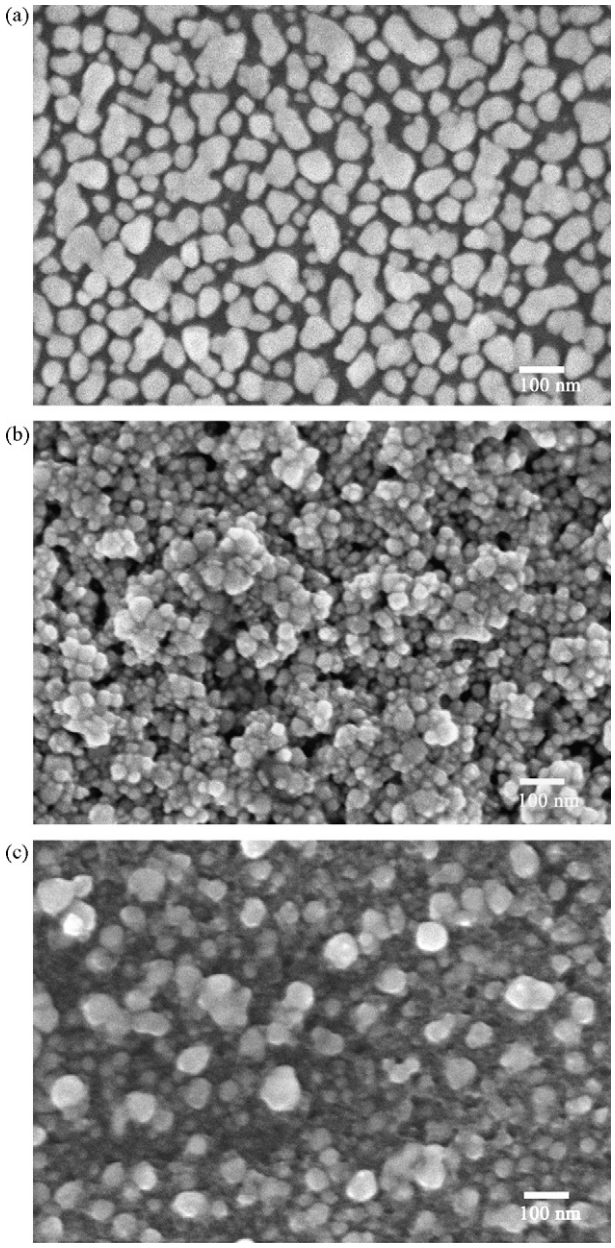

Fig. 1. SEM images of AgNPs coated PSi substrates prepared from methods A (a), B (b) and C (c), where bright particles are AgNPs and the supporting background is porous silicon.

As shown in Fig. 3, mass spectra of PEG 400, TPyP, oxytocin, and PEG 2300 are obvious on all three substrates prepared by methods A, B, and C at their nanomole quantities (PEG 400 and PEG 2300 at 3 nmol and TPyP and oxytocin at 1 nmol, respectively). PEG polymers (PEG 400 and PEG 2300) demonstrate distribution of oligomers with an adjacent repeat unit CH_2CH_2O (m/z 44). The molecule-related ions appear as $[M+Na]^+$ and/or $[M+K]^+$, which

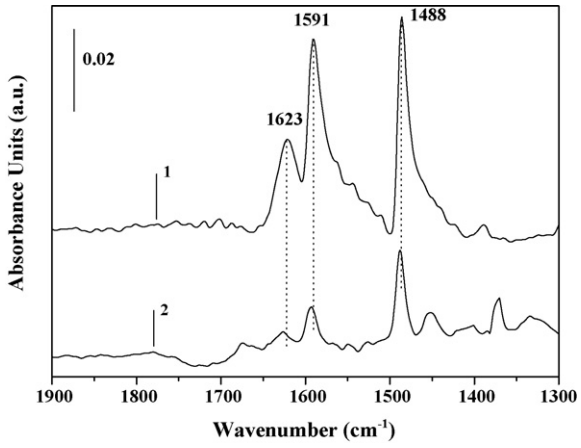

Fig. 2. FTIR spectra of 4-ATP self-assembled monolayers prepared with method B (1) and method C (2).

correspond to adducts of molecules and ubiquitous sodium or potassium ions. For TPyP, not only the protonated ion $[TPyP+H]^+$, but also the adduct of silver ion $[TPyP+Ag]^+$ was present, whereas oxytocin was ionized as $[oxytocin\text{-}H_2+Na]^+$ only (oxytocin is a peptide with two cysteine ends and it is in the disulphide form (oxytocin-H_2) in solution).

There are two reasons for adding 4-ATP to the plating solution: first, the reduction and deposition of silver from silver nitrate solution is too fast to be controlled and the complexation of thiol compound 4-ATP with Ag^+ slows down the reduction and therefore makes the size and deposition of nanoparticles controllable, secondly, 4-ATP SAMs can partly serve as matrix to help the desorption/ionization of target molecules. For example, 4-ATP-capped gold nanoparticles (AuNPs) were used to desorb and ionize biomolecules, insulin (m/z ~ 6 kDa) and cytochrome c (m/z ~ 12,400 Da), for LDI MS [28]. From Fig. 3, 4-ATP-capped silver particles from both methods B and C enhanced the LDI signal. Although 4-ATP-related ions were observed in the low-mass region, $[4\text{-ATP-H}]^+$ (m/z 124), $[4\text{-ATP}+Ag]^+$ (m/z 231), and other 4-ATP-related ions, mass spectra of target molecules revealed better S/N ratios and resolutions on 4-ATP capped surfaces. Furthermore, the useful analyte mass range is increased in PEG 2300 of Fig. 3, where more symmetric sinusoidal shape of mass distribution can be found by methods B and C than by method A. And the laser power was also lower than by method A. It suggests that the capping of 4-ATP here be an efficient matrix. Method C provides a medium S/N ratio and resolution among the three methods. Probably the number of AgNPs plays some role. The main reason for presenting method C is the shorter plating time (10 min) for preparation of the substrate. A conclusion can be drawn, the larger the number of AgNPs deposited, the more efficient the substrate for LDI. Additionally, we found that 4-ATP capped substrates stored for a month in air showed no significant degradation in sensitivity and resolution for LDI MS.

For comparison, the aforementioned analytes have also been measured on freshly prepared porous silicon substrates in our case and on standard stainless steel targets with traditional matrix, α-cyano-4-hydroxycinnamic acid (CHCA). Fig. 4A and B shows the mass spectra of TPyP and oxytocin detected on porous silicon with the same input of samples. But no signals were detected for PEG 400 and PEG 2300 on our PSi substrates prepared from our supplier's silicon wafers under the etching conditions described in

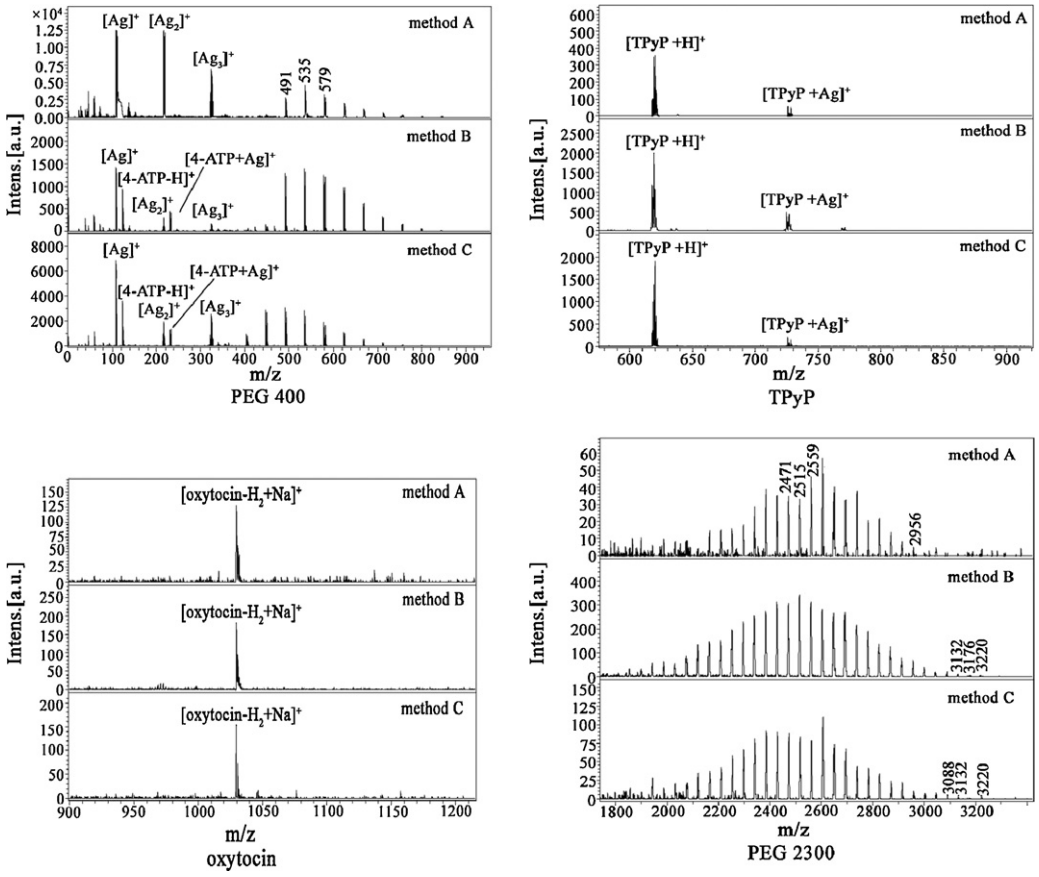

Fig. 3. Mass spectra of PEG 400, TPyP, oxytocin, and PEG 2300 obtained using AgNPs and 4-ATP/AgNPs deposited PSi substrates prepared with methods A, B and C.

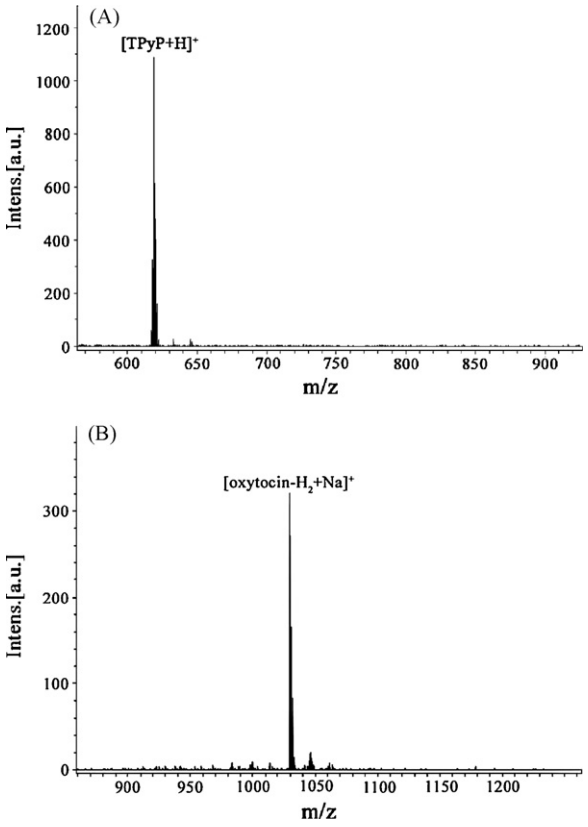

Fig. 4. Mass spectra of TPyP (A) and oxytocin (B) from our freshly prepared PSi substrates.

Section 2. As reported, silicon crystal orientation, dopant level, etching conditions such as current density, etching solution, and etching time are all parameters affecting the morphology and surface structure of porous silicon [12,43–48], and therefore the DIOS performance severely [12]. In our case, SEM observations revealed a porous layer with a pore diameter of 4–10 nm and a layer depth of 1–2 μm [49]. This kind of porous silicon layer produced in our lab is DIOS-inactive for PEG 400 and PEG 2300. It indicates that the DIOS method needs careful screening of silicon resources and etching parameters for some specific molecules. However the silver-plated PSi substrate presents much higher tolerance for many kinds of molecules.

By dropping the same amount of samples mixed with the organic matrix CHCA on a standard stainless steel target individually, we obtained the mass spectra of PEG 400, TPyP, oxytocin and PEG 2300 in Fig. 5, respectively. Comparing Figs. 3–5, the resolutions for the four analytes were comparable with each other. However, as we described in the introduction, MALDI possesses the phenomena of 'sweet spot' and 'dead spot', where the signal varies largely from one spot to another spot. Under the above measurement parameters, the relative standard deviations for PEG 400, TPyP, oxytocin and PEG 2300 over 5 spots are 45%, 49%, 33%, and 42%, respectively. While the signal on 4-ATP/AgNPs coated PSi substrates has less variations. The relative standard deviations for PEG 400, TPyP, oxytocin and PEG 2300 over 5 spots are 21%, 10%, 16%, and 8%, respectively, which improved the measurement repetition greatly. The 4-ATP/AgNPs coated PSi approach might be of a potential method for better quantification in LDI MS.

The above examples illustrate that the AgNPs and 4-ATP/AgNPs coated PSi substrates are quite effective in generating intact gas-phase ions by LDI. Thus, the major role of AgNPs is to provide assistance in desorption of analytes into their gas phase. As reported, ultra-fine nanoparticles with a diameter less than the laser beam wavelength were used for LDI and enhanced the mass signal. The mechanism of the ultrafine powder in assisting the LDI of analyte molecules is related to the scattering of the laser light between particles, resulting in high absorption and low reflection [14,50]. The energy dispersion within the particles is low, and thus it promotes a rapid heating, which is critical for generating intact gas-phase molecules [50]. The size of AgNPs in Fig. 1 is smaller than the laser wavelength 337 nm. In our case, when a laser irradiates AgNPs, the laser energy is absorbed by the illuminated AgNPs quickly and part of the light would be scattered in the void space between the adjacent particles. Since the laser energy is quickly absorbed by particles it will not effectively dissipate into the bulk plate. As a result, the particles irradiated by the laser pulse are rapidly heated, which in turn vaporize the analyte molecules and ionize them. In some cases, the higher laser power causes fragmentation of analytes, which suggests the character of a thermal driving force. AgNPs prepared from method B in Fig. 1(b) exhibited a three-dimensional stacking structure. In this case, the laser energy absorbed by nanoparticles can be rapidly dissipated to the adjacent un-illuminated nanoparticles because of their much larger surface contacts with each other. Energy transfer between nanoparticles likely occurs by conductive AgNPs and a lower laser power is needed to vaporize the analytes for detection. The mechanism can be partly supported from the easier desorption/ionization of analytes by method B than by methods A and C.

4-ATP is 'matrix-like' and is a small substituted aromatic molecule that absorbs energy in the ultraviolet. In our experiment, the SAMs might act as a matrix via three possible routes for LDI [27]: (1) AgNPs deposited PSi absorbs the laser energy and thermally desorbs 4-ATP, which then acts as a matrix for the analyte, (2) the SAMs matrix absorbs the light, transfer the energy to AgNPs and analytes, and desorbs and ionizes the analytes, and (3) combination of the above two modes. Thus, we can explain why the 4-ATP/AgNPs coated PSi substrate can enhance the LDI efficiency, decrease the ion fragmentation and the laser energy, and increase the useful analyte mass range effectively.

The detection limits of TPyP with S/N ≥ 3, oxytocin with S/N ≥ 3, and PEG 400 and PEG 2300 with visible sinusoidal shapes of mass distribution on the 4-ATP/AgNPs coated PSi substrate fabricated with method B were examined and compared to DIOS and classical CHCA MALDI methods in Table 1. TPyP and oxytocin are small molecules and can be easily detected with all three methods. Both 4-ATP/AgNPs and CHCA methods can obtain lower detection limits for TPyP to femtomoles and for oxytocin to subpicomoles, while DIOS can only reach detection limits to picomoles. However synthetic polymers, PEG 400 and PEG 2300, did not give any signals on our DIOS substrate, but presented detection limits to picomoles by means of 4-ATP/AgNPs and CHCA methods. We showed the detection limit spectra of PEG 400 and PEG 2300 in Fig. 6 on our 4-ATP/AgNPs substrate, where the mass distribution can be still observed.

Table 1
Comparison of the detection limits of TPyP, oxytocin, PEG 400, and PEG 2300 with three methods: 4-ATP/AgNPs coated PSi substrate, classical CHCA method, and DIOS method based on our freshly etched PSi.

Analyte	Detection limit		
	4-ATP/AgNPs	CHCA	DIOS
TPyP	5.2 fmol	1.0 fmol	1.3 pmol
Oxytocin	0.4 pmol	0.4 pmol	1.5 pmol
PEG 400	3.0 pmol	3.0 pmol	–
PEG 2300	30 pmol	0.3 pmol	–

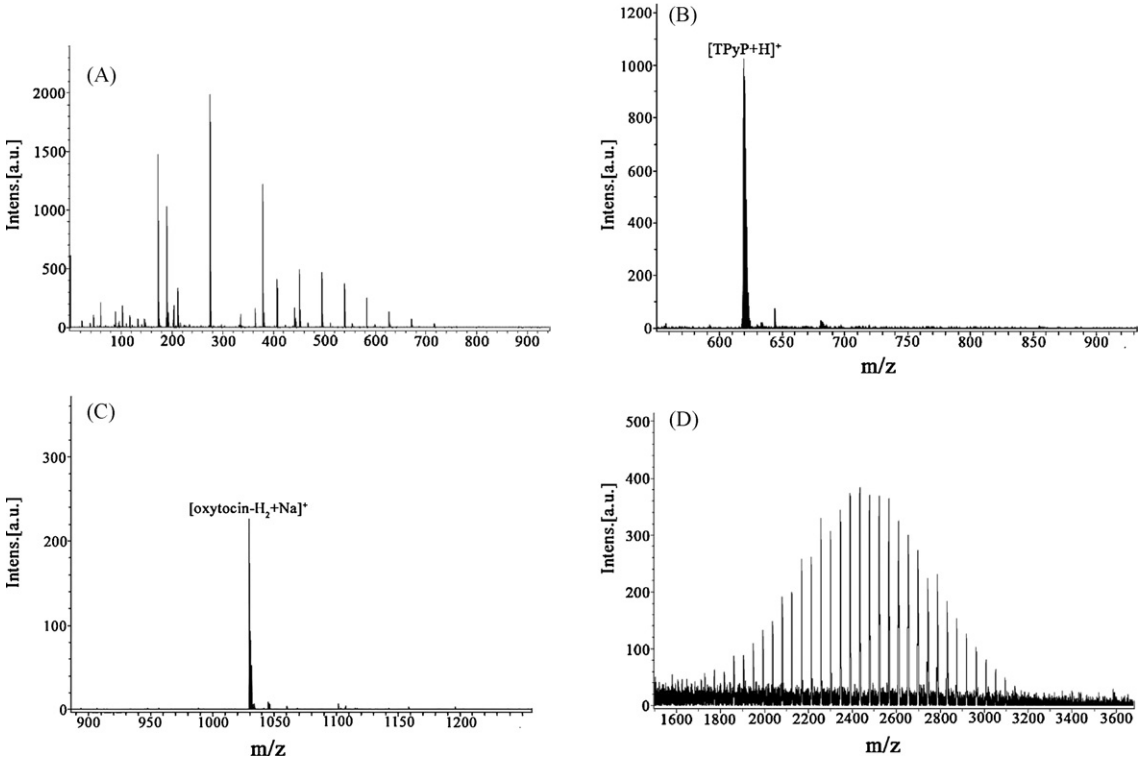

Fig. 5. Spectra of PEG 400, TPyP, oxytocin, and PEG 2300 on a standard stainless steel target by addition of the organic matrix CHCA.

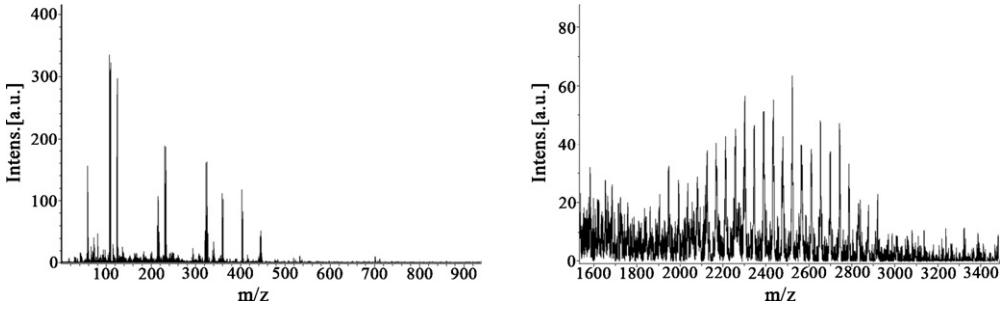

Fig. 6. Mass spectra of PEG 400 (left, 3.0 pmol) and PEG 2300 (right, 30 pmol) on the 4-ATP/AgNPs coated PSi substrate prepared from method B.

4. Conclusions

AgNPs deposited PSi substrates have been used for surface-enhanced Raman scattering (SERS) with varying degrees of success. As we show here, this type of substrates are also excellent candidates for LDI substrates. They were successfully used to analyze synthetic polymers, low molecular weight organic compounds, and small peptide molecules by LDI MS. Even more the 4-ATP involved plating method was established to control the deposition size and speed of AgNPs on PSi substrates. And the resulted 4-ATP capped substrate was more efficient for LDI than a substrate just covered by the naked AgNPs, with higher ionization efficiency, less fragmentation, and more useful analyte mass information. The silver-deposited surface presents much higher tolerance for many kinds of molecules than with DIOS. Compared to the traditional matrix method, it simplifies the sample preparation (matrix-free-like) and homogenizes the sample spread over the spot for better and more even mass signals. It can obtain limits of detection to several femtomoles for TPyP, subpicomoles for oxytocin, and picomoles for PEG 400 and PEG 2300, which are comparable to the traditional matrix method. And a variety of SAM surfaces will bring a wide range of biomedical applications in proteomics.

Acknowledgments

The authors thank the anonymous reviewers for their careful reading, thorough and diligent reviews. We thank Prof. Yan-Chun Tang in the Institute of Molecular Medicine and Prof. Zhen Shen in the State Key Laboratory of Coordination Chemistry at Nanjing Univ. for providing the analytes kindly, and Mrs. Yu-Hua Mei for her technical helps. We are grateful to the financial support of the National Basic Research Program of China, No. 2007CB925101, NSFC, No. 20721002 and No. 20571042, and an open research fund of state key laboratory of bioelectronics, Southeast University.

References

[1] A. Vertes, G. Irinyi, R. Gijbels, Anal. Chem. 65 (17) (1993) 2389.
[2] D.S. Peterson, Mass Spectrom. Rev. 26 (1) (2007) 19.
[3] Y.C. Chen, J.Y. Wu, Rapid Commun. Mass Spectrom. 15 (20) (2001) 1899.
[4] S.Y. Xu, Y.F. Li, H.F. Zou, J.S. Qiu, Z. Guo, B.C. Guo, Anal. Chem. 75 (22) (2003) 6191.

[5] W.Y. Chen, L.S. Wang, H.T. Chiu, Y.C. Chen, C.Y. Lee, J. Am. Soc. Mass Spectrom. 15 (11) (2004) 1629.
[6] C.S. Pan, S.Y. Xu, L.G. Hu, X.Y. Su, J.J. Ou, H.F. Zou, Z. Guo, Y. Zhang, B.C. Guo, J. Am. Soc. Mass Spectrom. 16 (6) (2005) 883.
[7] C.S. Pan, S.Y. Xu, H.F. Zou, Z. Guo, Y. Zhang, B.C. Guo, J. Am. Soc. Mass Spectrom. 16 (2) (2005) 263.
[8] S.F. Ren, Y.L. Guo, Rapid Commun. Mass Spectrom. 19 (2) (2005) 255.
[9] S.F. Ren, L. Zhang, Z.H. Cheng, Y.L. Guo, J. Am. Soc. Mass Spectrom. 16 (3) (2005) 333.
[10] J. Wei, J.M. Buriak, G. Siuzdak, Nature 399 (6733) (1999) 243.
[11] J.D. Cuiffi, D.J. Hayes, S.J. Fonash, K.N. Brown, A.D. Jones, Anal. Chem. 73 (6) (2001) 1292.
[12] Z.X. Shen, J.J. Thomas, C. Averbuj, K.M. Broo, M. Engelhard, J.E. Crowell, M.G. Finn, G. Siuzdak, Anal. Chem. 73 (3) (2001) 612.
[13] N.H. Finkel, B.G. Prevo, O.D. Velev, L. He, Anal. Chem. 77 (4) (2005) 1088.
[14] K. Tanaka, H. Waki, Y. Ido, S. Akita, Y. Yoshida, T. Yoshida, T. Matsuo, Rapid Commun. Mass Spectrom. 2 (8) (1988) 151.
[15] T. Yalcin, W.E. Wallace, C.M. Guttman, L. Li, Anal. Chem. 74 (18) (2002) 4750.
[16] W.Y. Chen, Y.C. Chen, Anal. Chem. 75 (16) (2003) 4223.
[17] C.T. Chen, Y.C. Chen, Anal. Chem. 77 (18) (2005) 5912.
[18] T. Kinumi, T. Saisu, M. Takayama, H. Niwa, J. Mass Spectrom. 35 (3) (2000) 417.
[19] M. Schürenberg, K. Dreisewerd, F. Hillenkamp, Anal. Chem. 71 (1) (1999) 221.
[20] J.A. McLean, K.A. Stumpo, D.H. Russell, J. Am. Chem. Soc. 127 (15) (2005) 5304.
[21] Y.F. Huang, H.T. Chang, Anal. Chem. 78 (5) (2006) 1485.
[22] C.L. Su, W.L. Tseng, Anal. Chem. 79 (4) (2007) 1626.
[23] E.P.C. Lai, S. Owega, R. Kulczycki, J. Mass Spectrom. 33 (6) (1998) 554.
[24] K. Shrivas, H.F. Wu, Anal. Chem. 80 (7) (2008) 2583.
[25] B.N.Y. Vanderpuije, G. Han, V.M. Rotello, R.W. Vachet, Anal. Chem. 78 (15) (2006) 5491.
[26] A.H. Brockman, B.S. Dodd, R. Orlando, Anal. Chem. 69 (22) (1997) 4716.
[27] S. Mouradian, C.M. Nelson, L.M. Smith, J. Am. Chem. Soc. 118 (36) (1996) 8639.
[28] E.T. Castellana, D.H. Russell, Nano Lett. 7 (10) (2007) 3023.
[29] M.J. Dale, R. Knochenumss, R. Zenobi, Anal. Chem. 68 (19) (1996) 3321.
[30] M.J. Dale, R. Knochenumss, R. Zenobi, Rapid Commun. Mass Spectrom. 11 (1) (1997) 136.
[31] Q.C. Zhang, H.F. Zou, Z. Guo, Q. Zhang, X.M. Chen, J.Y. Ni, Rapid Commun. Mass Spectrom. 15 (3) (2001) 217.
[32] Z. Guo, A.A.A. Ganawi, Q. Liu, L. He, Anal. Bioanal. Chem. 384 (3) (2006) 584.
[33] S. Kaneco, Y.S. Chen, P. Westerhoff, J.C. Crittenden, Scripta Mater. 56 (5) (2007) 373.
[34] H.P. Wu, C.L. Su, H.C. Chang, W.L. Tseng, Anal. Chem. 79 (16) (2007) 6215.
[35] T.T. Hoang, Y.F. Chen, S.W. May, R.F. Browner, Anal. Chem. 76 (7) (2004) 2062.
[36] S. Alimpiev, A. Grechnikov, J. Sunner, V. Karavanskii, Y. Simanovsky, S. Zhabin, S. Nikiforov, J. Chem. Phys. 128 (1) (2008) 014711.
[37] M. Han, J. Sunner, J. Am. Soc. Mass Spectrom. 11 (7) (2000) 644.
[38] E.P. Go, J.V. Apon, G. Luo, A. Saghatelian, R.H. Daniels, V. Sahi, R. Dubrow, B.F. Cravatt, A. Vertes, G. Siuzdak, Anal. Chem. 77 (6) (2005) 1641.
[39] S. Chan, S. Kwon, T.W. Koo, L.P. Lee, A.A. Berlin, Adv. Mater. 15 (19) (2003) 1595.
[40] I. Coultard, S. Degen, Y.J. Zhu, T.K. Sham, Can. J. Chem. 76 (11) (1998) 1707.
[41] T. Sakka, T. Tsuboi, Y.H. Ogata, J. Porous Mater. 7 (1–3) (2000) 397.
[42] L.L. Sun, G. Wei, Y.H. Song, Z.G. Liu, L. Wang, Z. Li, Appl. Surf. Sci. 252 (14) (2006) 4969.
[43] L.T. Canham, Properties of Porous Silicon, Institute of Electrical Engineers, London, 1997.
[44] A. Janshoff, K.-P.S. Dancil, C. Steinem, D.P. Greiner, V.S.-Y. Lin, C. Gurtner, K. Motesharei, M.J. Sailor, M.R. Ghadiri, J. Am. Chem. Soc. 120 (46) (1998) 12108.
[45] C.-H. Lin, S.-C. Lee, Y.-F. Chen, J. Appl. Phys. 75 (12) (1994) 7728.
[46] P.C. Searson, J.M. Macaulay, F.M. Ross, J. Appl. Phys. 72 (1) (1992) 253.
[47] R.L. Smith, S.D. Collins, J. Appl. Phys. 71 (8) (1992) R1.
[48] M. Thoenissen, M.G. Berger, R. Arens-Fischer, O. Glueck, M. Krueger, H. Lueth, Thin Solid Films 276 (1) (1996) 21.
[49] D.-J. Guo, S.-J. Xiao, B. Xia, S. Wei, J. Pei, Y. Pan, X.-Z. You, Z.-Z. Gu, Z. Lu, J. Phys. Chem. B 109 (43) (2005) 20620.
[50] S. Kawabata, A. Bowdler, K. Tanaka, Proceedings of 46th ASMS Conference on Mass Spectrometry and Allied Topics, 1998, p. 1011.